On the Static Fatigue Limit for Soda-Lime-Silica Glass*

by

M. W. Davis,

J. S. Wasylyk,

and

Russell D. Southwick

AMERICAN GLASS RESEARCH, INC.
Butler, Pennsylvania

It is well known that sustained, sub-critical tensile loads on glass articles may result in the slow growth of pre-existing flaws in the glass surface. It is necessary that the flaw-containing glass surface be exposed to water (liquid or vapor) for such slow crack growth to occur. This process is commonly known as "static fatigue". When a flaw has grown to a certain critical extent, the glass fails in an unstable manner.

Earlier work has shown that the critical flaw size necessary to cause failure is dependent upon the level of the applied stress. For a given pre-existing flaw size, the present study shows that there is a minimum applied stress level below which slow crack growth will not occur. This threshold level of applied stress or static fatigue limit has been found to be a constant fraction (0.27) of the inert strength of the pre-existing flaw. This criterion in terms of applied stress is equivalent to a stress-intensity factor K_0 equal to 27 percent of the fracture toughness K_{IC} of the glass.

*Presented at German Glass Technology Society, Augsburg,, Germany, May 24-26, 1982.
Published in *Glastechnische Berichte*, 56 (1983) No. 5.

Alternatively, the static fatigue limit can now be expressed in terms of the particular time to failure when the applied stress is equal to this threshold stress level. We define a static fatigue endurance duration to exist at that point. The endurance duration represents the longest possible time to failure, and has been found to be dependent on the pre-existing initial flaw depth in a given environment. Examples are given of the application of these two equivalent concepts of a static fatigue limit to the practical use of glass as an engineering material.

INTRODUCTION

When a glass object is subjected to a sufficient tensile load over a period of time in the presence of an active environment such as water, failure may occur at applied stress levels below those necessary to produce failure in an inert or water-free environment. The strength decrease due to such loading in an active environment is commonly referred to as static fatigue. The fatigue phenomenon results from the slow growth or extension of mechanically produced flaws in the glass surface.

In the presence of sufficient tensile stresses, an active water environment may lead to rupture of atomic bonds at the highly stressed flaw tip through a process commonly referred to as stress corrosion, effectively increasing the flaw depth, reducing strength. If such flaws

are subjected to an active environment in the absence of tensile stresses, the flaws may age or become rounded due to chemical interactions between the glass at the flaw tip and the environment. As the flaws age, the corresponding strength of the object is increased. Aging and fatigue have both been shown to be time-dependent phenomena.

When aging proceeds at a faster rate than static fatigue, a fraction of the strength loss produced by the introduction of a given flaw may be recovered. When the rate of slow crack growth or static fatigue exceeds that of aging, continued strength loss results. When the two competing processes counterbalance one another, neither strength loss through fatigue nor strength recovery due to aging occurs. Since the fatigue phenomenon is associated with the presence of a tension stress, the counterbalancing of the fatigue and aging phenomena implies that, for a given initial flaw size, there exists an applied stress level below which crack growth or fatigue will not occur, i.e., a fatigue limit will be established. The concept of an "endurance limit", i.e., survival under load for a minimum period of time would guarantee survival under the same load for a much longer time period, was first advanced by Holland[1] in 1936.

Alternatively, as first expressed by Mould and Southwick[2] in their pioneering work on static fatigue, a normalized strength under constant tensile loading conditions may be defined as the ratio between the applied stress at which a given flaw will fail in an active environment

(denoted by σ_A) and the inert strength of that same flaw determined in an inert environment (denoted by σ_N). When the normalized strengths were plotted as a function of the time to failure, t_F, a series of fatigue curves resulted as seen in Figure 1. The lower strength curves showed some evidence of approaching an asymptotic normalized strength at relatively longer times to failure, i.e., at a normalized strength of circa 0.20 in Mould and Southwick's original work. The implications of the existence of a fatigue limit are of importance to the design and application of brittle materials such as glasses which are subject to the static fatigue phenomenon.

At this point, it is important to emphasize that the fatigue limit cannot be expressed as a single unambiguous stress value. The fatigue limit or failure criterion in a given environment is determined relative to a given initial flaw size which exists at the beginning of the static fatigue tensile loading interval, and which also has associated with it a specific value of σ_N, the inert strength.

Since Mould and Southwick's original fatigue studies, more recent investigators have produced fatigue limit data for soda-lime-silica glasses under a variety of experimental conditions as seen in Table I. Ritter and Sherbourne[3] determined that a fatigue limit exists for a soda-lime-silica composition at a normalized strength of 0.32 in a liquid water environment, and a slightly higher fatigue limit value in a 50%

relative humidity environment. Pavelchek and Doremus[4] found a fatigue limit at a normalized strength of 0.40 for abraded soda-lime-silica glass in a 23°C liquid water environment. Charles and Hillig[5] recorded a normalized strength of 0.15 at the fatigue limit for a similar soda-lime-silica glass, while Wilkins and Dutton[6] determined a static fatigue limit of 0.17 for abraded soda-lime-silica specimens at a temperature of 400°C.

The range over which unstable crack propagation will occur may also be expressed in terms of the stress intensity factor K_I. Weiderhorn and Bolz[7] determined the fatigue limit for soda-lime-silica glass in water at 23°C under double cantilever load conditions to be given by a K_I value of 0.25 MPa-$m^{1/2}$. Simmons and Freiman[8] reported a fatigue limit value under similar conditions, of 0.27 MPa-$m^{1/2}$. Assuming a fracture toughness K_{IC} = 0.8 MPa-$m^{1/2}$ for soda-lime-silica glass, the above fatigue limit stress intensity values may be converted to normalized strengths (σ_A/σ_N) of 0.31 and 0.34, respectively.

It was our purpose to experimentally determine the existence of the static fatigue limit for mechanically abraded soda-lime-silica glass specimens under constant loading conditions. Our data show that a fatigue limit exists at a normalized strength of 0.27. Previous experimenters have shown the existence of a fatigue limit expressed in terms

of applied stress and the inert strengths. It is our further purpose to show that a reduced time-to-failure parameter may be used as a new, alternative failure criterion at the static fatigue limit. The ratio of time to failure to initial flaw size (t_f/a_i) at the fatigue limit is uniquely determined and may be used as an alternative failure criterion for a specific environment. This endurance duration, if exceeded by a given article, ensures, that under a constant applied stress, failure will not occur regardless of how long the load remains in place.

THEORETICAL

Many of the recent advances in the understanding of glass strength and glass fracture processes have been due to the development of fracture mechanics as applied to brittle materials. The basic principles and underlying assumptions used in fracture mechanical analysis of glass fracture processes have been described in numerous articles in the glass literature, and will not be repeated here.

The static fatigue limit or failure criterion is the applied stress level which, if exceeded, will lead to failure. It will have a unique value for any given initial flaw size and may be expressed as a fraction of the inert strength associated with that flaw.

A functional relationship may be derived expressing the region I crack propagation velocity V in the K-V diagram illustrated in Figure 2, in terms of the crack opening stress intensity factor K_I and the appropriate crack propagation constants A and N, which are temperature and environmentally dependent. The region I crack velocity may be written as:

$$V = da/dt = AK_I^N \tag{1}$$

where V is the crack velocity, a is the crack depth and, t is the time of load duration.

At failure, the following integral expression results from manipulation and substitution in the above expression:

$$\int_{a_i}^{a_c} a^{-N/2}\, da = A(\sigma y)^N \int_{o}^{t_f} dt \tag{2}$$

where t_f is the time to failure, a_i and a_c are the initial and critical flaw depths, respectively, and y is a constant relating to flaw geometry.

Performing the appropriate integrations in equation 2 yields an equation for the time to failure t_f in terms of the previously defined parameters and the failure stress σ:

$$t_f = \frac{a_c^{1-N/2} - a_i^{1-N/2}}{(1-N/2)A(\sigma y)^N} \tag{3}$$

$$\frac{t_f}{a_i} = \frac{2}{(N-2)A} \frac{1}{K_{IC}^N} \left[\left(\frac{a_c}{a_i} \right)^{N/2} - 1 \right] \tag{3a}$$

If $(a_c/a_i)^{N/2} >> 1$, this means with $N \geq 17$ for applied stress levels below approximately 80% of the inert strength, the above expression may be simplified and rearranged to give the following expression which is linear in $\ln (t_f/a_i)$ and $\ln (a_i/a_c)^{1/2}$.

$$\ln \left[\left(\frac{a_i}{a_c} \right) \right]^{1/2} = C - \frac{1}{N} \ln \left[\left(\frac{t_f}{a_i} \right) \right] \tag{4}$$

where:

$$C = \frac{1}{N} \ln \left[\left(\frac{N-2}{2} \right) A K_{IC}^N \right] \tag{5}$$

K_{IC} = material fracture toughness

The functional form of the above expression is seen to be similar to the universal static fatigue curve determined by Mould and Southwick[2] as seen in Figure 3, in which the ratios of fatigue strength σ normalized by the inert strength σ_N or σ/σ_N were plotted using a reduced time to failure $(t/t_{0.5})$ as the independent variable. The normalizing factor or characteristic time $t_{0.5}$ was the time to failure for each individual set of fatigue data, at which the normalized strength equaled 0.5. Such normalization allowed the generation of a single universal fatigue curve of the form

$$\sigma/\sigma_N = f(t/t_{0.5}) \qquad (6)$$

The characteristic time was found to have a functional dependence on the inert strength as seen in Figure 4. For both point and line flaws, the characteristic time was found to increase with the reciprocal liquid nitrogen strength. That relationship shows that a specimen with a low inert strength or a large initial flaw size fatigues less rapidly than a specimen containing a smaller initial flaw size and having a higher strength.

The relationship between the normalized strength (σ/σ_N) of Mould and Southwick, the stress intensity ratio (K_I/K_{IC}), and the initial and critical flaw depths, a_i and a_c, respectively, may be seen from the following:

$$\frac{\sigma}{\sigma_N} = \frac{K_I}{K_{IC}} = \left(\frac{a_i}{a_c}\right)^{1/2} \tag{7}$$

Thus, the normalized flaw depth, $(a_i/a_c)^{1/2}$ in equation (4) may be replaced either with a normalized strength term (σ/σ_N), as in Mould and Southwick's universal fatigue curve, or with a ratio of normalized stress intensities K_I/K_{IC}.

A separate and unique fatigue curve will then be established for each glass composition, dependent on the nature at the fatiguing environment and the fatigue environment temperature.

At the fatigue limit, the normalized strength is defined as a constant given by

$$\ln\left[\left(\frac{a_i}{a_c}\right)^{1/2}\right] = \text{constant } \gamma \tag{8}$$

Static Fatigue Limit

The constancy of $\ln[(a_i/a_c)^{1/2}]$ at the fatigue limit in turn suggests that the reduced time-to-failure parameter (t_f/a_i) may be expressed in terms of the material and crack propagation parameters K_{IC}, A and N in the following manner

$$\left(t_f / a_i \right) = \exp \left[N(C-Y) \right] \quad (9)$$

Static Fatigue Limit

where C is as expressed in equation (5).

Thus, a comparison of the experimental $\ln(t_f/a_i)$ values and those calculated for a given environment and temperature should prove the validity of using (t_f/a_i) as a new, alternative failure criterion.

EXPERIMENTAL METHODS

Static fatigue data were generated in room temperature water by simultaneously subjecting a series of mechanically abraded microscope slides of a soda-lime-silica composition as listed in Table II, to constant, long load duration four-point bending. A testing device was constructed which was capable of being submerged in a deionized water bath of the desired temperature. These specimens were loaded in four-point bending. Since no two specimens had exactly the same thickness, provisions were made to allow variable weights to be added to each test station to generate the desired tensile stress on the abraded face of each glass

slide. Microswitches were fashioned at each individual station to electronically record the time to failure of each specimen.

A sample size of twenty specimens was used for each of the static fatigue samples at a given applied stress level as well as for each of the control or inert strength samples.

Prior to fatigue testing, a central 1 cm^2 section of each slide, from a group of 40, was given a uniform grit-blast abrasion treatment. Silicon carbide grit, passing a 50 mesh but retained on a 60 mesh standard sieve, was entrained in an 80 psig pressure nitrogen gas stream and directed at each slide. The specimens were aged by immersion in 23°C deionized water for a 24-hour period for the 23°C fatigue tests. The samples for the 60°C fatigue tests were aged by being placed in water initially at 23°C, and then heated to 60°C over a two-hour period. The samples were then maintained in the 60°C water for an additional 22 hours. The abraded slides were then randomly selected and separated into two groups for each set of experimental fatigue data.

The first set of abraded slides was used for the constant load static fatigue testing, while the second set constituted a control sample whose inert strengths were determined by testing the specimens in liquid nitrogen conditions. The inert strengths of the control specimen

set were used to determine the initial flaw size distribution in each set of abraded samples from the relationship

$$a_i = \left(\frac{K_{IC}}{y\sigma_N} \right)^2 \tag{10}$$

where $y = \sqrt{\pi}$.

The applied stress level used in each constant load static fatigue test was a specified fraction of the median inert strengths of each of the corresponding control sets. Initially, an applied stress level was chosen to be a sufficiently high fraction of the median inert strength, such that a large number of the specimens in each sample set failed. Subsequent sets were tested at lower applied stress levels, corresponding to smaller fractions of the median inert strength. As a result, smaller numbers of each sample set failed.

The fatigue test duration for each level of applied stress was determined from the fatigue and control sample failure probability distributions. A maximum projected time to failure, beyond that of the last failing fatigue specimen, was obtained from the fatigue data at a failure probability matching that of the highest inert control sample

strength. The applied stresses in the fatigue determinations were maintained for durations at least twice the longest expected time to failure based on the last-failing specimen of the fatigue set at each applied stress level.

EXPERIMENTAL RESULTS

Inert strengths were determined from liquid nitrogen strength data as illustrated in Figure 5, arranged in cumulative failure probability form. The times to failure in the active water environment were also plotted on a cumulative probability plot. The normalized strengths, used to determine the fatigue limit in each case, were found by dividing the fatigue strength data fitted to a linear regression at a given probability by the similarly determined inert strengths at the identical probability in the inert strength control sample. In those cases where not all the fatigue specimens failed, the data were assigned probabilities based on the full set of 20 samples with the times-to-failure distribution plots being truncated at the last failing specimen.

Since the static fatigue limit has been defined as the applied stress level for a given initial flaw size below which static fatigue will not occur, the failure criterion for a given environment was associated with the smallest normalized strength at each applied stress level at which failure occurred.

The above procedure was performed on data obtained for constant applied load levels at varying fractions of the median inert strength levels for eight sample sets held in deionized water at 23°C as seen in Table III, and six corresponding sets in deionized water at 60°C shown in Table IV, to determine temperature sensitivity.

The first four columns in each of the tables list the constant applied stress, the number of specimens failing at each applied load level, the equivalent inert strength in liquid nitrogen, and the derived normalized strength at the fatigue limit for each data set. The time to failure for the last failing specimen in each test is given in Column 5 while the calculated values of initial flaw size a_i are given in Column 6. This latter column was obtained from the inert strengths of the control samples. The reduced time to failure at the fatigue limit is listed as $\ln(t_f/a_i)$ in Column 7.

DISCUSSION

For a given unimodal distribution of initial flaw depths a_i, the number of failing specimens in a constant load fatigue strength determination should increase linearly with increasing applied stress. If a static fatigue failure limit exists at a unique value of the normalized

strength, then as the applied stress is decreased, the number of failing specimens in the distribution having normalized strengths greater than or equal to the static fatigue limit should also decrease. This behavior was observed as seen in Figure 6 for specimens in water at both 23°C and 60°C. The average normalized strengths at the static fatigue limit for both environment temperatures resulted in essentially the same normalized stress values of 0.273 and 0.271, with standard deviations of 0.009 in both cases, respectively.

Further confirmation of the existence of a static fatigue limit at a constant normalized strength was obtained from the relationship between the inert strengths of the last failing specimen in each fatigue group and the applied stress level. Again, for a unimodal distribution of initial flaw depths, the inert strengths associated with the last failing specimen at a given applied stress level should increase linearly with increasing applied stress regardless of environmental temperature. Such behavior was observed as seen in Figure 7.

The natural logarithms of the mean values of the experimentally determined (t_f/a_i) parameter at the fatigue limit were 22.27 and 20.12, with standard deviations of 0.674 and 0.607, for the 23°C and 60°C water environments, respectively. Using A and N data listed in Table V as determined in other unpublished fatigue studies, calculated $\ln(t_f/a_i)$ values of 22.55 and 20.20 were obtained for 23° and 60°C, respectively. These values compare very favorably with the experimental data seen in Tables II and III.

The experimental reduced times to failure at the fatigue limit were markedly different and were found to be markedly dependent on environmental temperature. The reduced time-to-failure parameter at the fatigue limit was significantly shorter in the 60°C, than in the 23°C water environment, the relationship between the two parameters being the following:

$$\underset{\substack{\text{Static Fatigue Limit} \\ (60°C)}}{(t_f/a_i)} = 0.156 \underset{\substack{\text{Static Fatigue Limit} \\ (23°C)}}{(t_f/a_i)} \qquad (11)$$

Since the static fatigue limit has been uniquely determined at a constant value of normalized strength for a water environment at two different temperatures, static fatigue curves determined in different environments will accordingly produce a different value for the corresponding reduced time parameter (t_f/a_i) at the fatigue limit. Those values of (t_f/a_i) may be used to determine a maximum time to failure for a given initial flaw size, which if exceeded without specimen failure will insure that the object containing that flaw will never fail, as long as the same environment and constant loading conditions are maintained.

Each of the above (t_f/a_i) constants for a particular environment may then be used to predict the maximum expected time to failure under constant loading conditions for a given initial flaw size. Should the flaw not grow by fatiguing to critical dimensions a_c in the calculated time t_f, one may be assured that the article containing the flaw will never break under the specified loading conditions.

The alternative failure criterion is to assure that the applied stress level in a glass object, containing a flaw of initial size a_i corresponding to an inert strength σ_N, is maintained at or less than 0.27 σ_N. If this condition is maintained, the flaw will not fatigue and failure will not occur.

The point of particular interest here is that the failure criterion may then be defined, once an initial flaw size and environmental condition is specified, in terms of <u>either</u> the applied stress or the time to failure. If an applied stress level is maintained at or less than 27% of the inert strength of the maximum initial size flaw in the sample, or if the object survives constant loading for a minimum time as determined by the environmental parameters A and N and fracture toughness K_{IC}, one will be assured that fatigue and failure will not occur under the stated load.

CONCLUSIONS

The two major goals of this study were to theoretically model and experimentally determine the static fatigue limit for a given soda-lime-silica composition in tensile loading for a water environment.

It has been shown that one failure criterion for a particular soda-lime-silica glass composition in water may be expressed in terms of the normalized strength ratio $\sigma/\sigma_N = 0.27$. If applied stresses are maintained at less than 27% of the corresponding inert strength, failure will not occur under the conditions specified, regardless of load duration.

Alternatively, should an article containing an initial flaw size, a_i, be stressed and survive a time under load t_f given by

$$t_f \geq \Theta a_i \tag{12}$$

where Θ is an environmentally determined constant derived from Equation (9), failure will not occur.

At the fatigue limit, the competing rate processes of aging (which increases strength) and fatigue (which decreases strength) offset each other. Below the fatigue limit, aging predominates, with the resultant effect that failure will not occur due to slow crack growth.

TABLE I

Static Fatigue Limit Literature Data Summary

Investigators	Reference No.	Glass★	Fatigue Environment	σ_A/σ_N @ Fatigue Limit
Mould/Southwick	2	Soda-lime-silicate	23°C - Water	~0.20
Ritter/Sherburne	3	Soda-lime-silicate	23°C - Water	0.32
			23°C - 50% RH	0.34
Pavelchek/Doremus	4	Soda-lime-silicate	23°C - 50% RH*	~0.42
		Soda-lime-silicate	23°C - 50% RH	0.23
Charles/Hillig	5	Soda-lime-silicate	23°C - Water	~0.15+
Wilkins/Dutton	6	Soda-lime-silicate	400°C - air⊛	~0.17
Wiederhorn/Bolz	7	Soda-lime-silicate	25°C - Water	~(0.31)†
Simmons/Freiman	8	Soda-lime-silicate	22°C - Water	(0.34)†

★ See listed references for exact glass compositions and experimental conditions.
* Following either a one hour 400° or 500°C soak treatment.
+ Estimate based on Mould and Southwick data.
⊛ Strength tested at room temperature following a 24 hour 400°C annealing treatment while under tensile load.
† Derived from stress intensity factor data.

Table II

Glass Composition used in the Static Fatigue Limit study.

SiO_2	72 w/o
Na_2O	14
CaO	7
MgO	4
Al_2O_3	2
K_2O	1

Table III

Static Fatigue Data Summary
in 23°C Water Environment

Applied Stress (MPa)	Specimens Failing	Equivalent Inert Strength (MPa)	Static Fatigue Limit	Time to Fail Last Failing Specimen (sec.)	Initial Flaw Depth (m)*	$\ln(t_f/a_i)$
25.42	19/20	87.93	0.289	1.044×10^5	2.635×10^{-5}	22.10
24.18	16/20	87/60	0.276	1.656×10^4	2.655×10^{-5}	22.55
23.40	16/20	83.42	0.281	9.360×10^4	2.927×10^{-5}	21.89
22.76	15/20	87.19	0.261	2.988×10^5	2.680×10^{-5}	23.13
22.45	9/20	81.78	0.274	2.160×10^5	3.046×10^{-5}	22.68
21.55	7/20	80.34	0.268	4.320×10^4	3.156×10^{-5}	21.04
20.82	3/20	78.27	0.266	1.044×10^5	3.325×10^{-5}	21.87
20.03	2/20	73.76	0.271	3.168×10^5	3.744×10^{-5}	22.86
			Mean = 0.273			Mean = 22.27
			$S_{\bar{x}} = 0.009$			$S_{\bar{x}} = 0.674$

*derived from $a_i = (K_{IC}/y\sigma_N)^2$; $K_{IC} = 0.8$ MPa-$m^{1/2}$; $y = \sqrt{\pi}$

Table IV

Static Fatigue Data Summary
in 60°C Water Environment

Applied Stress (MPa)	Specimens Failing	Equivalent Inert Strength (MPa)	Static Fatigue Limit	Time to Fail Last Failing Specimen (sec.)	Initial Flaw Depth (m)*	$\ln(t_f/a_i)$
25.24	12/20	88.96	0.283	7.20×10^{3}	2.574×10^{-5}	19.45
24.80	14/20	88.62	0.280	7.20×10^{3}	2.594×10^{-5}	19.44
24.14	12/18	91.03	0.265	2.52×10^{4}	2.458×10^{-5}	20.75
22.90	11/20	85.52	0.268	1.80×10^{4}	2.766×10^{-5}	20.29
22.05	5/20	80.69	0.273	1.44×10^{4}	3.129×10^{-5}	19.95
22.21	4/20	82.76	0.256	3.24×10^{4}	2.974×10^{-5}	20.81
			Mean = 0.271			Mean = 20.12
			$S_{\bar{x}} = 0.009$			$S_{\bar{x}} = 0.607$

*derived from $a_i = (K_{IC}/y\sigma_N)^2$; $K_{IC} = 0.8$ MPa-$m^{1/2}$: $y = \sqrt{\pi}$

Table V

Crack Propagation Constants

Fatigue Environment Temperature	Fatigue Environment	A	N
23°C	Water	1.714	16.349
60°C	Water	0.484	13.870

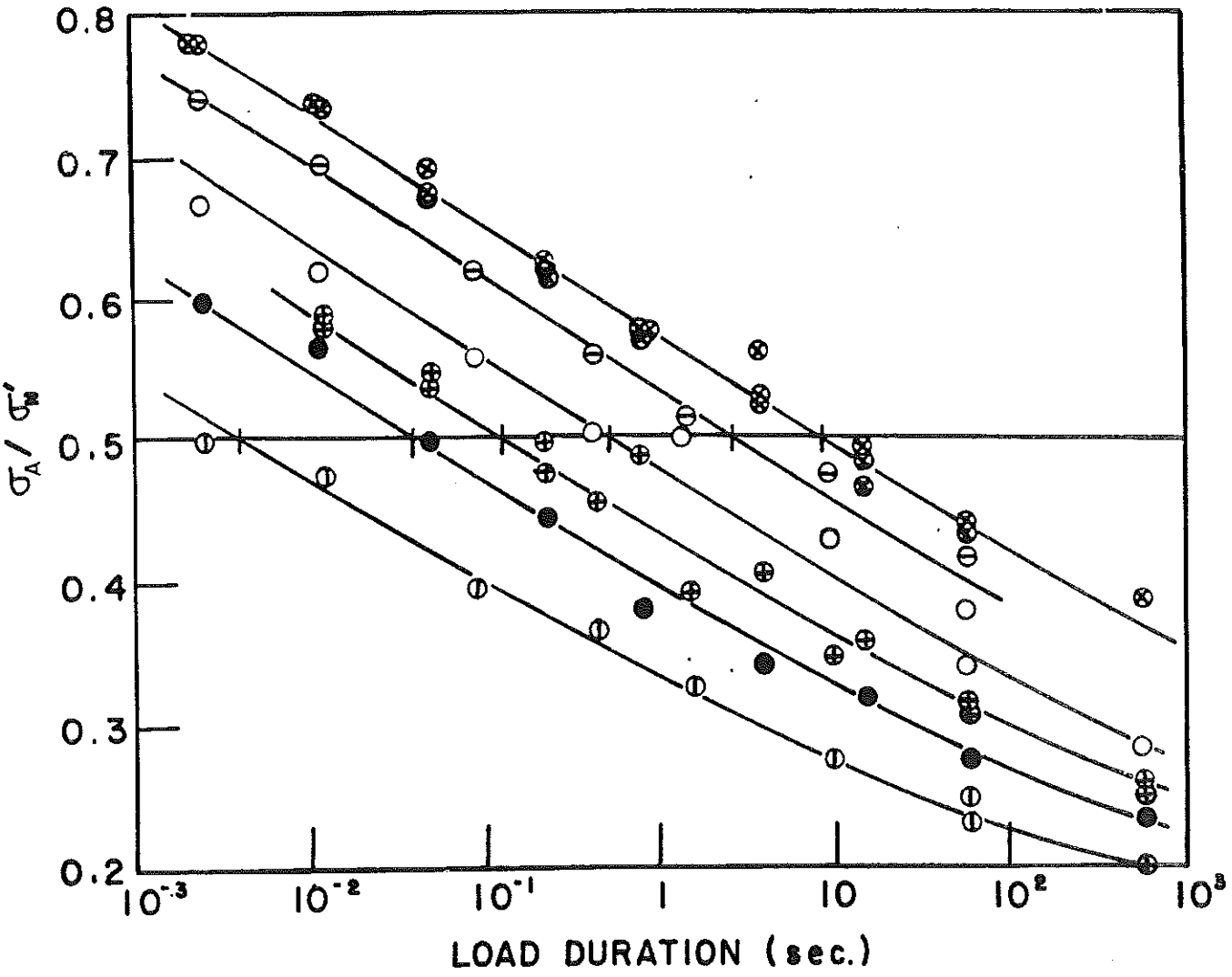

FIGURE 1

REDUCED STRENGTH Vs. LOAD DURATION (LOG SCALE) FOR VARIOUS ABRASIONS. STRENGTH VALUES, σ , DIVIDED BY ADJUSTED LIQUID NITROGEN STRENGTH (σ_N') FOR EACH ABRASION. VERTICAL MARKS ON $\sigma_A/\sigma_N' = 0.5$ LINE INDICATE VALUE OF $t_{0.5}$ FOR EACH CURVE.

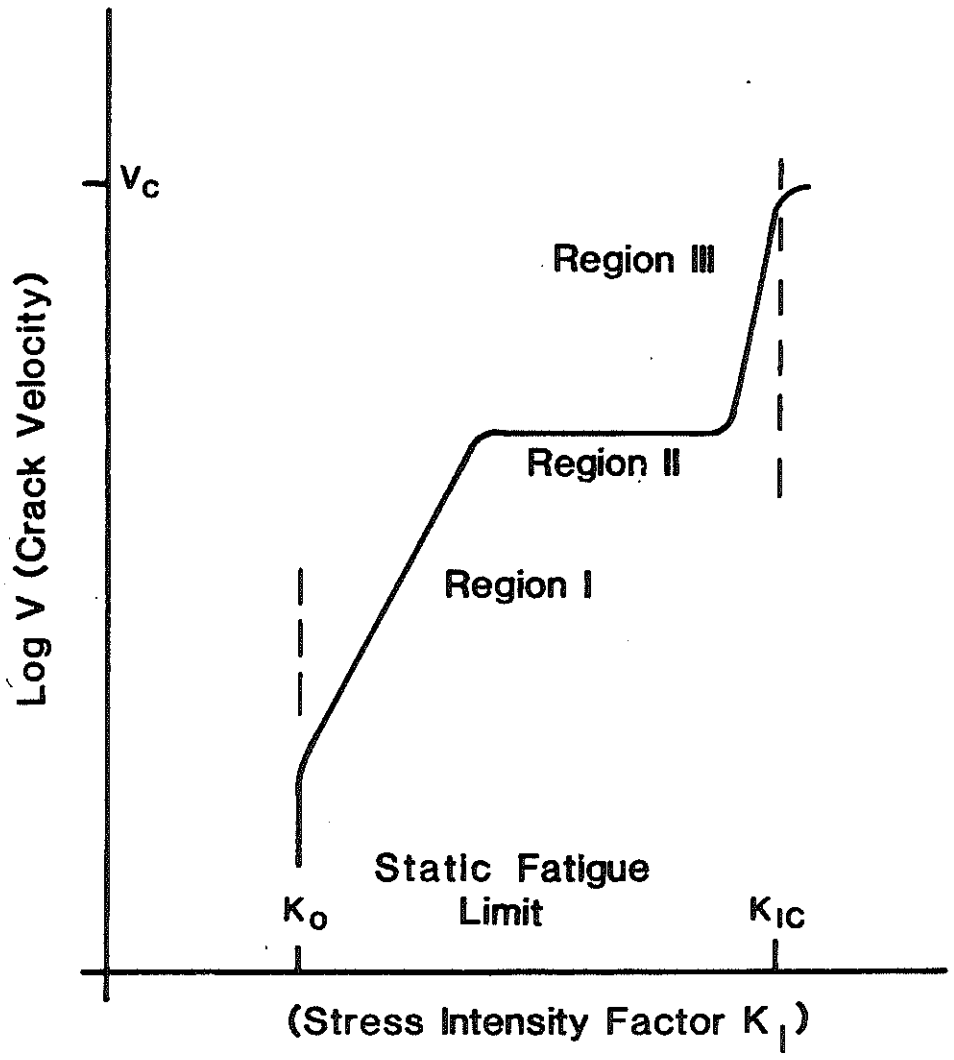

FIG. 2

Schematic Diagram outlining the Stress Intensity Factor - Crack Velocity Behavior of a Soda-lime-silica Glass

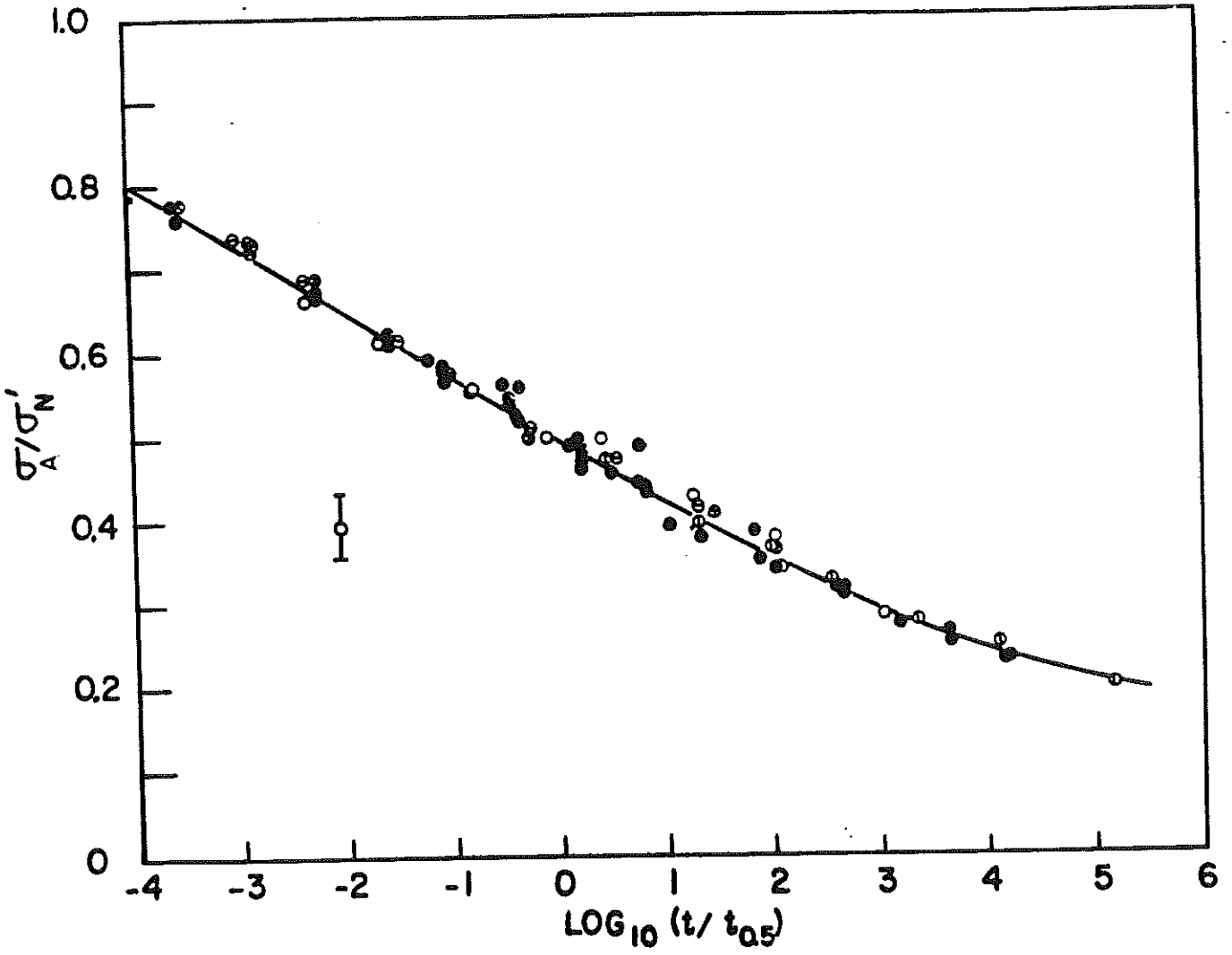

FIGURE 3

UNIVERSAL FATIGUE CURVE FOR VARIOUS ABRASIONS. STRENGTH DIVIDED BY LIQUID NITROGEN STRENGTH Vs. LOGARITHM OF LOAD DURATION DIVIDED BY $t_{0.5}$ FOR EACH ABRASION.

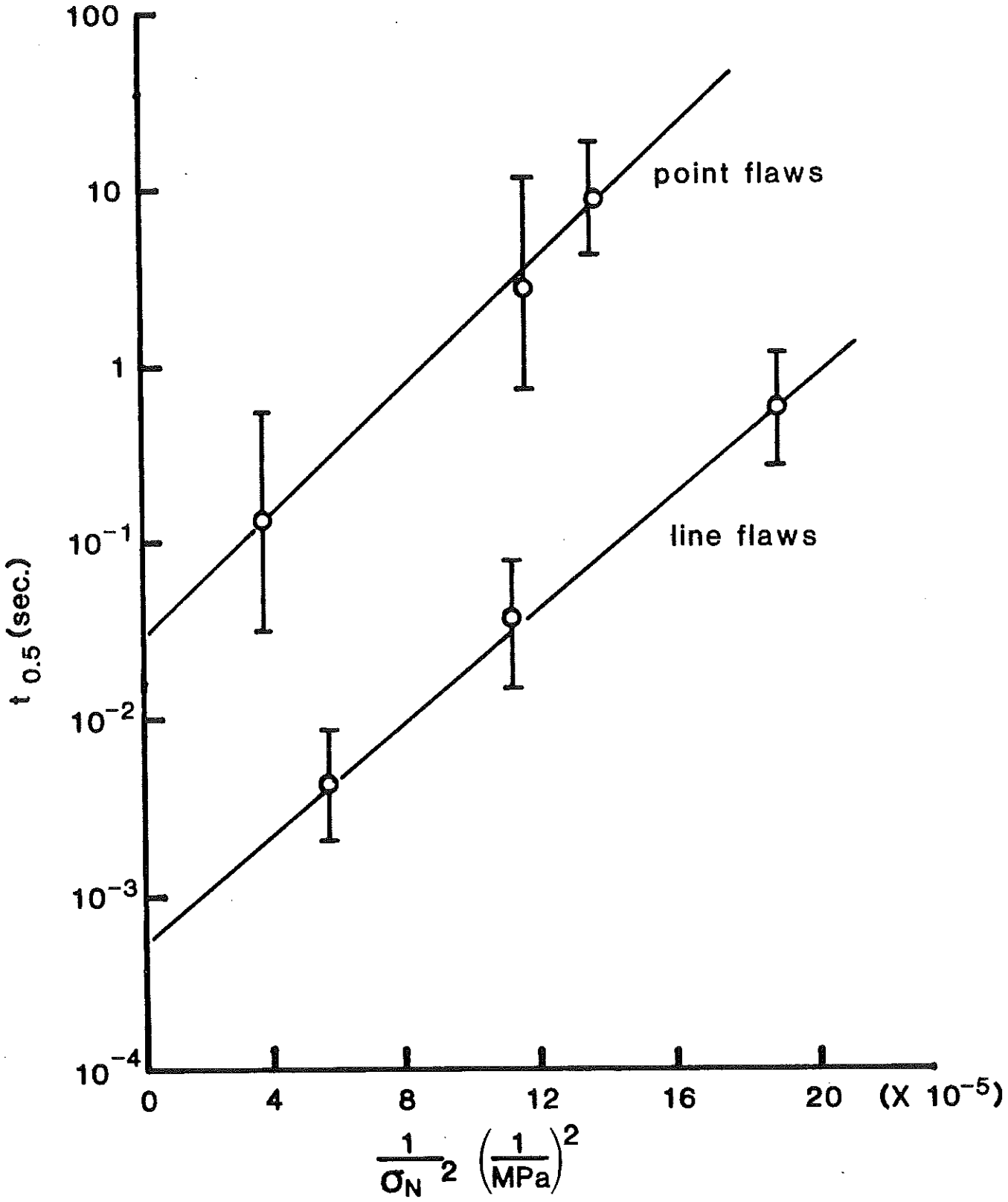

FIG. 4 Relationship between the characteristic time and reciprocal inert strength data.

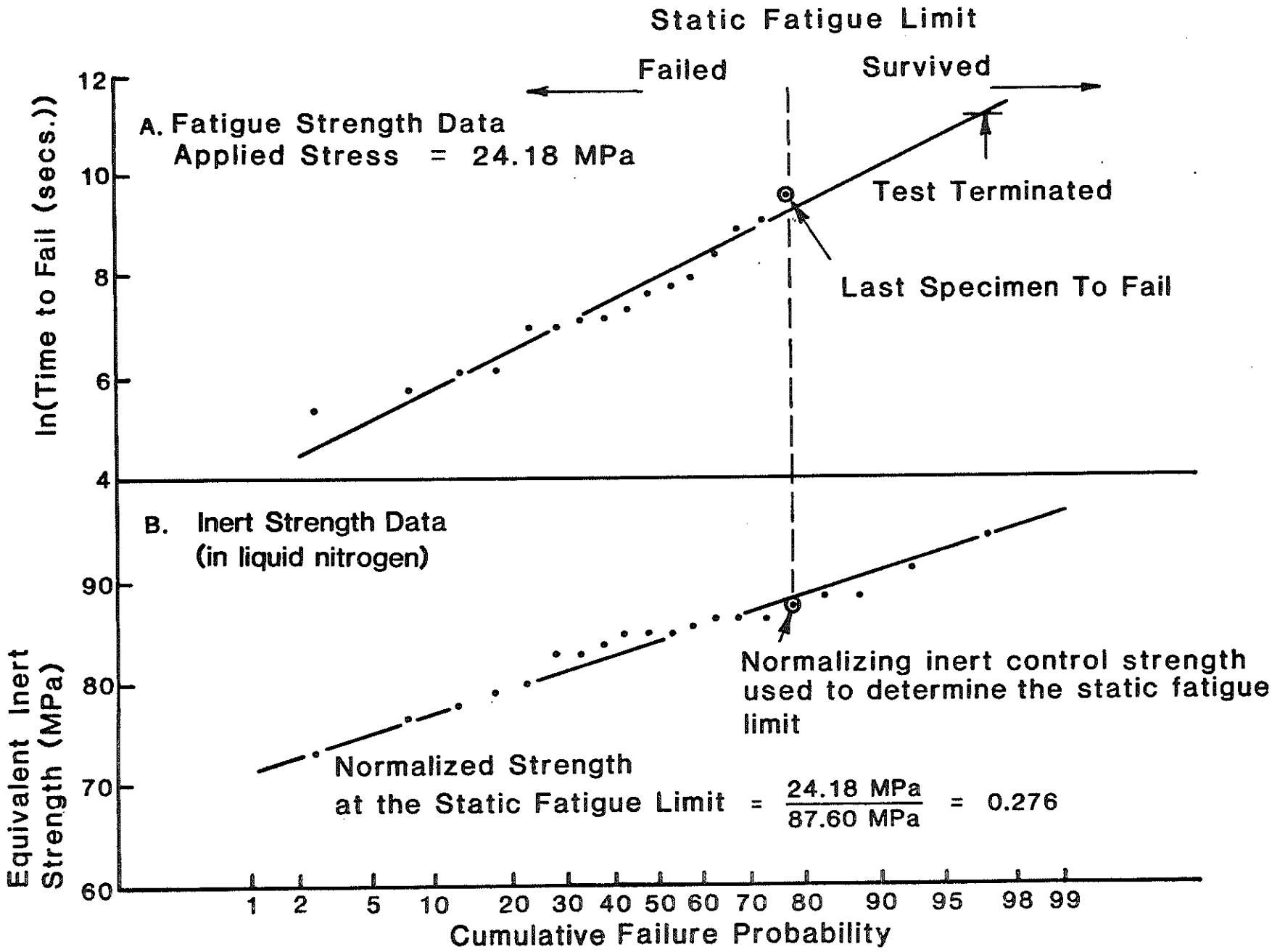

FIG. 5
Typical Fatigue/Inert Strength- Cumulative Failure Probability Plot

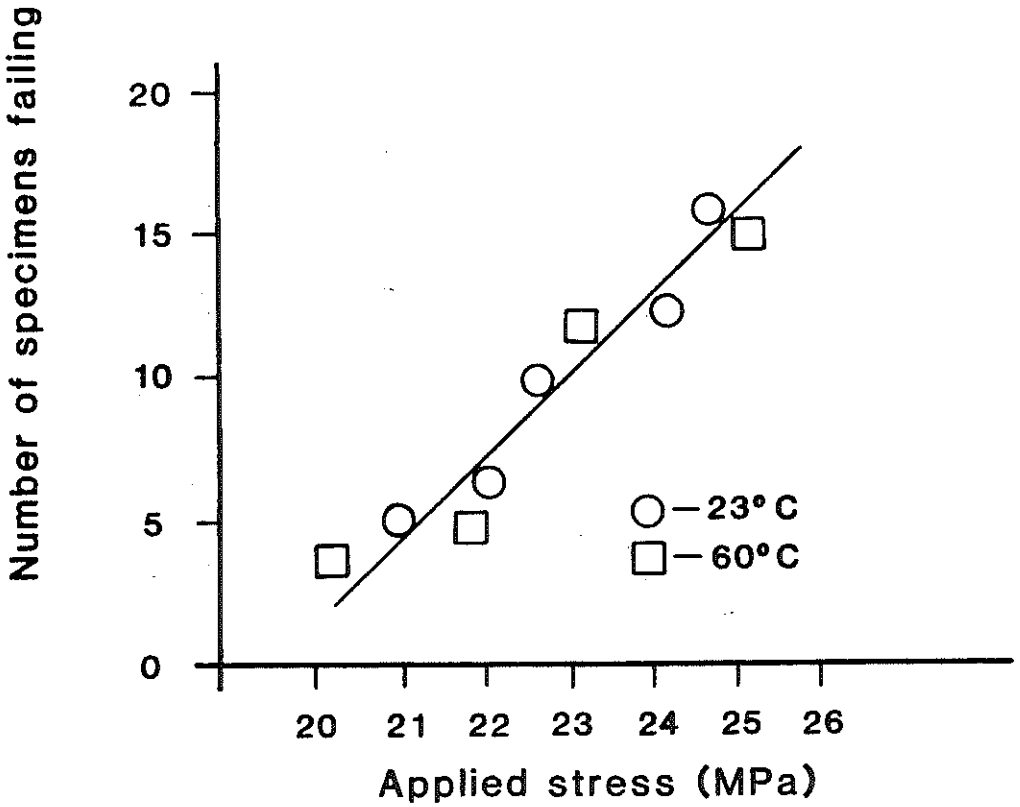

Fig.6
Relationship between the number of failing specimens and the applied stress level

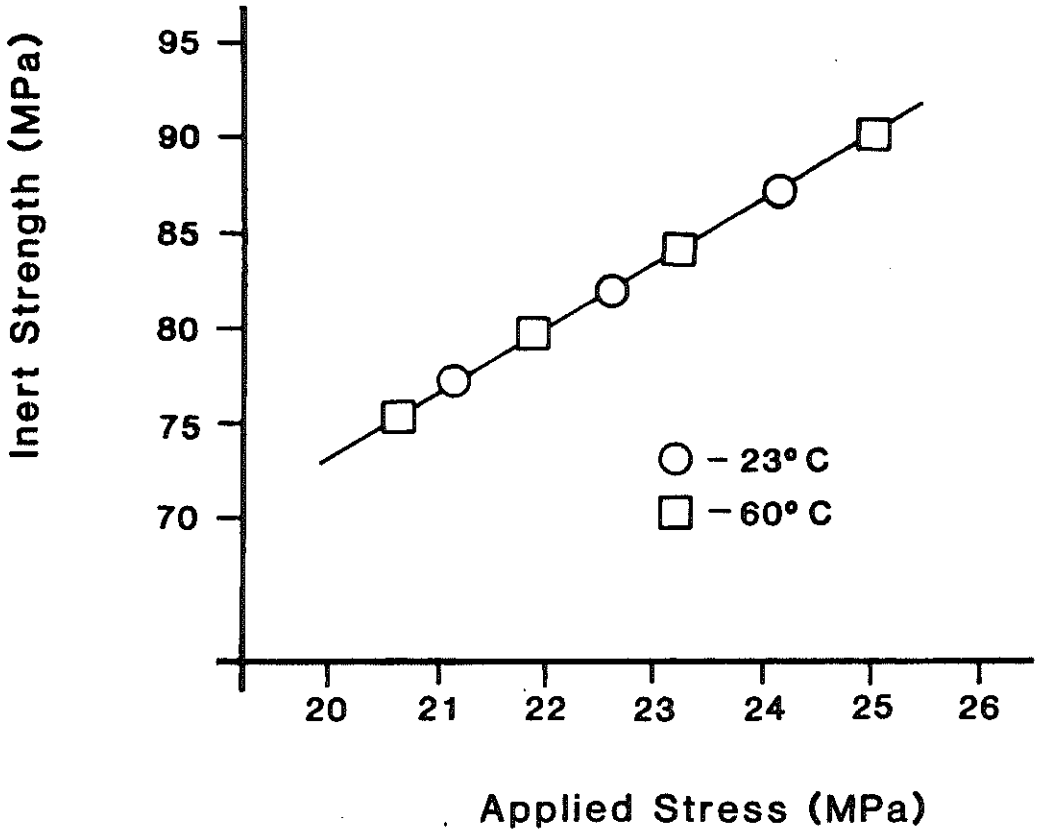

Fig.7
Relationship between the inert strength and the applied stress level.

REFERENCES

[1] A. J. Holland, "The Effect of Sustained Loading on the Breaking Strength of Glass", *The Glass Review*, 12 (9) 133-35 (1936).

[2] R. E. Mould and R. D. Southwick, "Strength and Static Fatigue of Abraded Glass under Controlled Ambient Conditions: II, Effect of Various Abrasions and the Universal Fatigue Curve", *J. Am. Ceram. Soc.*, 42 (12) 582-592 (1959).

[3] J. E. Ritter, Jr., and C. L. Sherburne, "Dynamic and Static Fatigue of Silicate Glasses", *J. Am. Ceram. Soc.*, 54 (12) 601-605 (1971).

[4] E. K. Pavelchek and R. H. Doremus, "Static Fatigue in Glass - A Reappraisal", *J. of Non-Crystalline Solids*, 20 305-321 (1976).

[5] R. J. Charles and W. B. Hillig; pp. 511-527 (in English) in Symposium sur la Resistance Mecanique du Verre et les Moyens de l'Ameliorer. Compte Rendu (Symposium on Mechanical Strength of Glass and Ways of Improving it, 1961). Union Scientifique Continentale du Verre, Charleroi, Belgium, 1962.

[6] B. J. S. Wilkins and R. Dutton, "Static Fatigue Limit with Particular Reference to Glass", *J. Am. Ceram. Soc.*, 59 (3-4) 108-112 (1976).

[7] S. M. Wiederhorn and L. H. Bolz, "Stress Corrosion and Static Fatigue of Glass", *J. Am. Ceram. Soc.*, 53 (10) 543-548 (1970).

[8] C. J. Simmons and S. W. Freiman, "Effect of Corrosion Processes on Subcritical Crack Growth in Glass", *J. Am. Ceram. Soc.*, 64 (11) 683-686 (1981).